Prenatal Exposure to Perfluoroalkyl Substances Associated with Increased Susceptibility to Liver Injury in Children

Table of Contents

Supporting Text S1: Quality assurance of PFAS assessment

Detailed information about the PFAS measurement quality assurance (QA) and quality control (QC) has been reported previously.(1) Briefly, internal QC samples were analyzed along with each batch of samples sent to NIPH to ensure high quality of the determinations. To monitor possible batch differences during the project, the results of all internal control samples were plotted in quality control charts per contaminant. The results were found satisfactory and no batch correction was applied. To ensure comparable results in PFAS assessment between RWTH at Aachen University (which conducted the assessment for INMA) and NIPH (which conducted the assessment for the other HELIX cohorts), 10 samples from INMA were assessed using the common HELIX protocol at NIPH and results were of similar magnitude and highly correlated (Spearman $r > 0.8$). Additionally, the NIPH laboratory participated three times in the “Arctic Monitoring and Assessment Program “Ring Test for Persistent Organic Pollutants in Human Serum” (AMAP) interlaboratory comparison study, with each round including 3 PFAS samples. The samples were spiked in a wide concentration range and Z-scores below 2 were obtained for all PFAS, except for PFUnDA in two samples. Moreover, 15 PFAS samples from 4 rounds of the AMAP interlaboratory comparison study were analyzed during the period when HELIX samples were analyzed, and the mean deviation from the assigned value varied between 8 and 17%.

Supporting Text S2: Bayesian Kernel Machine Regression (BKMR) modelling

The BKMR models used in our study are given by:

$$\Phi^{-1}(\mu_1) = h\,(\mathrm{PFOS}_i, \mathrm{PFOA}_i, \mathrm{PFNA}_i, \mathrm{PFHXS}_i, \mathrm{PFUnDA}_i) + \beta Z^T_{i1\ldots p} + \varepsilon_i \quad (1)$$

$$Y_i = h\,(\mathrm{PFOS}_i, \mathrm{PFOA}_i, \mathrm{PFNA}_i, \mathrm{PFHXS}_i, \mathrm{PFUnDA}_i) + \beta Z^T_{i1\ldots p} + \varepsilon_i \quad (2)$$

In equation (1), Φ^{-1} is the link function of the probit regression and $\mu_1 = P(Liver\ injury\ risk_i = 1)$ is the probability of the event "being at risk for liver injury" for each participant i $(i = 1, \ldots, 1105)$. Equation (1) was considered our main model. Probit model coefficients in this model were converted into odds ratios using $logit(\mu) = 1.6\,.\,\Phi^{-1}(\mu)$.(2) In equation (2), Y_i denotes the continuous liver enzyme concentrations $(\mathrm{ALT}_i,\ \mathrm{AST}_i, or\ \mathrm{GGT}_i)$ for each participant i. In both models, $h\,()$ denotes a high-dimensional exposure-response function for the PFAS mixture to be estimated, $Z^T_{i1\ldots p}$ denotes a set of p potential confounders, and $\varepsilon_i \sim \mathrm{N}\,(0, \sigma^2)$.

$h\,()$ can accommodate non-linearity and/or interaction among the mixture components and is estimated using a Gaussian kernel machine representation. This flexibly captures a wide range of underlying functional forms for $\mathrm{h}\,()$ and has been shown to work well in both simulation and epidemiologic studies. Intuitively, the Gaussian kernel assumes that two subjects with similar exposure profiles will have more similar liver outcome profiles, and this similarity is measured using the kernel function. BKMR was fit with the R package bkmr(2) using the Markov chain Monte Carlo algorithm with 10,000 iterations.(3) Once fitted, BKMR provides a posterior inclusion probability (PIP) for each of the exposures, which constitutes a measure of the relative importance of each exposure within the h function.(3)

Readers who are interested in BKMR are referred to Bob et al(3) that provides details about the statistical methodology. Moreover, previous analyses provide additional examples of BKMR implementation.(4, 5)

Supporting Text S3: xMWAS

xMWAS provides an automated framework for integrative and differential network analysis through 3 stages: 1) pairwise integrative analysis; 2) network visualization; and 3) differential network analysis.

In stage 1, we applied sparse Partial Least Squares regression, a dimension reduction technique, for pairwise data integration and for generating the association matrices between maternal blood PFAS and child serum metabolites in each group of children at high and low risk for liver injury. sPLS performs simultaneous data integration and variable selection using a LASSO penalty for the loading vectors. Within xMWAS, the *network()* function in the *mixOmics* package was used to generate the association score matrix, A_{XY}, between the matrices X (i.e., PFAS) and Y (i.e., metabolites), where the association score between variables X_i and Y_j is an approximation of their correlation coefficients determined using the PLS components and regression coefficients.(6-8) Student's t-test with an alpha level of 0.05 was used to evaluate the statistical significance of pairwise association scores; only associations with P <0.05 were used for downstream analysis.

Following the pairwise association analyses, an edge list matrix, L_e, was generated such that each row in L_e corresponded to an edge between PFAS and metabolites. Matrix L_e was then used to generate the integrative network graph, G=(V,E), where V corresponds to “nodes” (PFAS and metabolites) and E corresponds to edges or connections representing positive or negative associations of PFAS with metabolites. Network graphics in xMWAS are generated using the *igraph* package in R.(9)

In stage three of differential network analysis, the differential eigenvector centrality method was applied to identify nodes that underwent changes in their topological characteristics between the groups of children.(10, 11)

Readers who are interested in xMWAS are referred to Uppal et al(12) that provides details about statistical methodology. Moreover, previous analyses provide additional examples of xMWAS implementation.(13, 14)

Supporting Text S4: Latent integrated variable analysis (LUCIDus)

In the latent integrated variable analysis, PFAS mixture exposure was calculated as the sum of maternal plasma PFAS concentrations weighted by their posterior inclusion probabilities obtained from BKMR equation (1) to create a single variable capturing the relative importance of each PFAS within the mixture. In this analysis, we included the same set of covariates as the BKMR analysis for the association of the latent variables with liver injury risk. We obtained effect estimates for the association of estimated latent clusters with liver injury risk. For the estimation of the number of latent clusters, we used the Bayesian Information Criteria. The integrated analysis links the measured PFAS exposure variation (X) on liver injury risk (Y) via unmeasured and estimated subgroups (C).(15) In turn, the serum levels of metabolites (M) also characterize these unobserved (C) subgroups. Here, a model describing the liver injury risk (Y) as a function of cluster, C is $(\mu_Y) = \gamma_0 + \gamma_S C$, where γ_S represents the effect of each estimated cluster C, on the liver injury risk Y. The clusters are related to the metabolites as a multivariate normal model, $M \sim MVN(C\theta, \Sigma)$, where θ represents mean differences of the metabolite levels M by each cluster, and Σ is the covariance of the metabolites. The estimation of the clusters, C, follows a multinomial model with a linear predictor as a function of the PFAS exposures X, giving Pr(C=k | X, β), with corresponding effect estimates, β. Standard errors for parameters are estimated with a bootstrap procedure. Readers who are interested in LUCIDus are referred to Peng et al(15) that provides further details about statistical methodology. Moreover, previous analyses provide additional examples of LUCIDus implementation.(16-18)

Supporting references

1. Haug LS, Sakhi AK, Cequier E, Casas M, Maitre L, Basagana X, Andrusaityte S, et al. In-utero and childhood chemical exposome in six European mother-child cohorts. Environ Int 2018;121:751-763.
2. Bobb JF, Claus Henn B, Valeri L, Coull BA. Statistical software for analyzing the health effects of multiple concurrent exposures via Bayesian kernel machine regression. Environ Health 2018;17:67.
3. Bobb JF, Valeri L, Claus Henn B, Christiani DC, Wright RO, Mazumdar M, Godleski JJ, et al. Bayesian kernel machine regression for estimating the health effects of multi-pollutant mixtures. Biostatistics 2015;16:493-508.
4. Valeri L, Mazumdar MM, Bobb JF, Claus Henn B, Rodrigues E, Sharif OIA, Kile ML, et al. The Joint Effect of Prenatal Exposure to Metal Mixtures on Neurodevelopmental Outcomes at 20-40 Months of Age: Evidence from Rural Bangladesh. Environ Health Perspect 2017;125:067015.
5. Domingo-Relloso A, Grau-Perez M, Briongos-Figuero L, Gomez-Ariza JL, Garcia-Barrera T, Duenas-Laita A, Bobb JF, et al. The association of urine metals and metal mixtures with cardiovascular incidence in an adult population from Spain: the Hortega Follow-Up Study. Int J Epidemiol 2019.
6. Le Cao KA, Rossouw D, Robert-Granie C, Besse P. A sparse PLS for variable selection when integrating omics data. Stat Appl Genet Mol Biol 2008;7:Article 35.
7. Le Cao KA, Gonzalez I, Dejean S. integrOmics: an R package to unravel relationships between two omics datasets. Bioinformatics 2009;25:2855-2856.
8. Gonzalez I, Cao KA, Davis MJ, Dejean S. Visualising associations between paired 'omics' data sets. BioData Min 2012;5:19.
9. Csardi G, Nepusz T. The igraph software package for complex network research. InterJournal 2006;Complex Systems:1695.
10. Lichtblau Y, Zimmermann K, Haldemann B, Lenze D, Hummel M, Leser U. Comparative assessment of differential network analysis methods. Brief Bioinform 2017;18:837-850.
11. Odibat O, Reddy CK. Ranking differential hubs in gene co-expression networks. J Bioinform Comput Biol 2012;10:1240002.
12. Uppal K, Ma C, Go YM, Jones DP, Wren J. xMWAS: a data-driven integration and differential network analysis tool. Bioinformatics 2018;34:701-702.
13. Chandler JD, Hu X, Ko EJ, Park S, Fernandes J, Lee YT, Orr ML, et al. Low-dose cadmium potentiates lung inflammatory response to 2009 pandemic H1N1 influenza virus in mice. Environ Int 2019;127:720-729.
14. Hu X, Chandler JD, Fernandes J, Orr ML, Hao L, Uppal K, Neujahr DC, et al. Selenium supplementation prevents metabolic and transcriptomic responses to cadmium in mouse lung. Biochim Biophys Acta Gen Subj 2018.
15. Peng C, Wang J, Asante I, Louie S, Jin R, Chatzi L, Casey G, et al. A Latent Unknown Clustering Integrating Multi-Omics Data (LUCID) with Phenotypic Traits. Bioinformatics 2019.
16. Stratakis N, Conti DV, Borras E, Sabido E, Roumeliotaki T, Papadopoulou E, Agier L, et al. Association of Fish Consumption and Mercury Exposure During Pregnancy With Metabolic Health and Inflammatory Biomarkers in Children. JAMA Netw Open 2020;3:e201007.
17. Jin R, McConnell R, Catherine C, Xu S, Walker DI, Stratakis N, Jones DP, et al. Perfluoroalkyl Substances and Severity of Nonalcoholic Fatty Liver in Children: An Untargeted Metabolomics Approach. Environ Int 2019.
18. Alderete TL, Jin R, Walker DI, Valvi D, Chen Z, Jones DP, Peng C, et al. Perfluoroalkyl substances, metabolomic profiling, and alterations in glucose homeostasis among overweight and obese Hispanic children: A proof-of-concept analysis. Environ Int 2019;126:445-453.

Supporting Table S1. Distribution of maternal blood PFAS concentrations during pregnancy and their pairwise correlation coefficients

	PFOA	PFOS	PFHxS	PFNA	PFUnDA
> LOD (%)	99.7	100	97.5	97.9	95.4
Blood concentration, median (25^{th}-75^{th} percentile), ng/ml					
Overall	2.38 (1.45, 3.45)	6.74 (4.43, 10.35)	0.59 (0.34, 0.93)	0.72 (0.47, 1.11)	0.2 (0.13, 0.3)
BiB	1.93 (1.38, 2.82)	3.77 (2.36, 6.35)	0.43 (0.22, 0.91)	0.27 (0.17, 0.51)	0.04 (0.02, 0.1)
EDEN	3.51 (2.82, 4.56)	13.39 (9.31, 19.04)	1.01 (0.75, 1.52)	0.93 (0.7, 1.26)	0.16 (0.12, 0.21)
INMA	2.78 (1.99, 3.8)	6.19 (4.39, 8.07)	0.81 (0.58, 1.12)	0.8 (0.61, 1.07)	0.21 (0.14, 0.31)
KANC	1.03 (0.77, 1.49)	4.32 (3.1, 5.54)	0.34 (0.27, 0.47)	0.64 (0.44, 0.89)	0.2 (0.15, 0.27)
MoBa	2.15 (1.44, 3.11)	9.25 (6.73, 13.01)	0.65 (0.44, 0.9)	0.49 (0.36, 0.67)	0.25 (0.17, 0.36)
RHEA	2.33 (1.78, 3.22)	5.23 (4.01, 6.74)	0.27 (0.21, 0.41)	1.38 (1.1, 1.98)	0.28 (0.19, 0.39)
Spearman rho*					
PFOA	1.00	-	-	-	-
PFOS	0.61	1.00	-	-	-
PFHxS	0.65	0.70	1.00	-	-
PFNA	0.60	0.35	0.25	1.00	-
PFUnDA	0.18	0.26	0.11	0.42	1.00

LOD, limit of detection; PFHxS, perfluorohexane sulfonate; PFNA, perfluorononanoate; PFOA, perfluorooctanoate; PFOS, perfluorooctane sulfonate; PFUnDA, perfluoroundecanoate.

* Spearman rho was calculated for the overall study population and was based on $\log_2$-transformed PFAS concentrations

Supporting Table S2. Pairwise association scores between maternal blood PFAS concentrations in pregnancy and child serum metabolites in the integrative network of children at high liver injury risk

Metabolites	Class	PFOA	PFOS	PFHxS	PFNA	PFUnDA
Aspartate	AA	-0.16*	-0.19*	-0.24*	-0.02	0.01
Glutamate	AA	-0.16*	-0.18*	-0.21*	-0.06	-0.04
Glycine	AA	-0.10	-0.10	0.00	-0.19*	-0.18*
Isoleucine	AA	0.06	0.05	-0.11	0.25*	0.26*
Leucine	AA	0.05	0.05	-0.10	0.23*	0.23*
Lysine	AA	0.15*	0.17*	0.10	0.18*	0.16*
Phenylalanine	AA	0.01	0.00	-0.13	0.18*	0.19*
Serine	AA	-0.11	-0.14	-0.23*	0.05	0.07
Tryptophan	AA	0.10	0.10	-0.07	0.28*	0.28*
Tyrosine	AA	0.04	0.03	-0.08	0.17*	0.18*
Valine	AA	0.08	0.08	-0.08	0.26*	0.26*
C2	Acyl-Carn	0.02	0.01	-0.10	0.15*	0.16*
Acetylornithine	BA	0.02	0.01	-0.16*	0.23*	0.24*
Alpha-aminoadipic acid	BA	0.10	0.10	0.03	0.16*	0.15*
Creatinine	BA	0.16*	0.17*	0.09	0.20*	0.18*
Methionine sulfoxide	BA	-0.18*	-0.22*	-0.28*	-0.03	0.01
Taurine	BA	-0.13	-0.15*	-0.15*	-0.08	-0.06
Lyso-PC a C16:1	GP	0.10	0.10	0.04	0.14*	0.13
Lyso-PC a C18:1	GP	0.00	-0.02	-0.20*	0.24*	0.25*
Lyso-PC a C18:2	GP	-0.04	-0.06	-0.19*	0.14	0.16*
Lyso-PC a C20:3	GP	0.05	0.04	-0.17*	0.30*	0.31*
Lyso-PC a C20:4	GP	0.00	-0.01	-0.15*	0.19*	0.20*
PC aa C28:1	GP	0.14	0.15*	0.11	0.15*	0.13
PC aa C32:0	GP	-0.08	-0.10	-0.25*	0.15*	0.17*
PC aa C34:1	GP	0.02	0.00	-0.16*	0.22*	0.23*
PC aa C34:2	GP	-0.09	-0.11	-0.23*	0.09	0.12
PC aa C36:0	GP	0.13	0.15*	0.13	0.10	0.08
PC aa C36:1	GP	0.05	0.04	-0.10	0.22*	0.22*
PC aa C36:2	GP	-0.08	-0.09	-0.15*	0.03	0.04
PC aa C36:3	GP	-0.04	-0.06	-0.23*	0.19*	0.22*
PC aa C36:4	GP	-0.04	-0.06	-0.17*	0.12	0.13
PC aa C36:5	GP	0.07	0.10	0.20*	-0.09	-0.11
PC aa C36:6	GP	0.15*	0.18*	0.26*	-0.01	-0.04
PC aa C38:0	GP	0.14	0.16*	0.13	0.11	0.09
PC aa C38:3	GP	0.06	0.06	-0.03	0.15*	0.15*
PC aa C38:6	GP	0.15*	0.17*	0.21	0.04	0.01
PC aa C40:2	GP	-0.14*	-0.16*	-0.10	-0.16*	-0.14*
PC aa C40:4	GP	-0.08	-0.10	-0.16*	0.04	0.06

Supporting Table S2- continued.

Metabolites	Class	PFOA	PFOS	PFHxS	PFNA	PFUnDA
PC aa C40:5	GP	-0.11	-0.12	-0.05	-0.15*	-0.14*
PC aa C40:6	GP	0.13	0.16*	0.25*	-0.03	-0.06
PC ae C32:1	GP	0.04	0.04	-0.07	0.18*	0.18*
PC ae C32:2	GP	0.13	0.14*	0.07	0.18*	0.16*
PC ae C34:0	GP	0.09	0.09	-0.01	0.18*	0.18*
PC ae C34:1	GP	0.01	0.00	-0.15*	0.21*	0.22*
PC ae C34:2	GP	-0.02	-0.03	-0.15*	0.15*	0.17*
PC ae C36:0	GP	0.08	0.08	-0.04	0.21*	0.21*
PC ae C36:1	GP	0.05	0.05	-0.05	0.16*	0.16*
PC ae C36:3	GP	0.00	-0.02	-0.16*	0.19*	0.20*
PC ae C36:4	GP	0.09	0.08	-0.08	0.27*	0.27*
PC ae C36:5	GP	0.10	0.10	0.00	0.20*	0.20*
PC ae C38:0	GP	0.11	0.13	0.19*	-0.01	-0.04
PC ae C38:2	GP	-0.09	-0.11	-0.18*	0.04	0.06
PC ae C38:4	GP	0.05	0.05	-0.10	0.24*	0.24*
PC ae C38:5	GP	0.03	0.02	-0.13	0.22*	0.22*
PC ae C38:6	GP	0.16*	0.18*	0.12	0.18*	0.16*
PC ae C40:4	GP	-0.09	-0.11	-0.20*	0.06	0.08
PC ae C42:4	GP	-0.09	-0.10	-0.17*	0.03	0.05
H1	Hexose	0.10	0.10	-0.05	0.25*	0.24*
SM C16:1	SM	0.02	0.01	-0.08	0.14	0.14*
SM C18:0	SM	0.14	0.15*	0.05	0.22*	0.20*
SM C18:1	SM	0.12	0.13	0.03	0.21*	0.20*
SM C24:0	SM	-0.08	-0.10	-0.19*	0.07	0.09
SM (OH) C14:1	SM	0.12	0.13	0.07	0.15*	0.13
SM (OH) C16:1	SM	0.13	0.15*	0.10	0.15*	0.13
SM (OH) C22:1	SM	-0.02	-0.04	-0.21*	0.22*	0.24*
SM (OH) C24:1	SM	-0.01	-0.02	-0.13	0.15*	0.16*

Association scores were derived using sparse Partial Least Squares regression. AA, amino acid; Acyl-Carn, acylcarnitine; BA, biogenic amine; GP, glycerophospholipid; PC, phosphatidylcholine; PFHxS, perfluorohexane sulfonate; PFNA, perfluorononanoate; PFOA, perfluorooctanoate; PFOS, perfluorooctane sulfonate; PFUnDA, perfluoroundecanoate; SM, sphingomyelin.

* $P<0.05$

Supporting Table S3. Pairwise association scores between maternal blood PFAS concentrations in pregnancy and child serum metabolites in the integrative network of children at low liver injury risk

	Class	PFOA	PFOS	PFHxS	PFNA	PFUnDA
Isoleucine	AA	0.05	0.00	-0.03	0.16*	0.11
Glutamate	AA	-0.24*	-0.32*	-0.30*	0.01	-0.02
Glutamine	AA	0.10	0.15*	0.08	0.03	0.05
Aspartate	AA	-0.01	-0.20*	-0.18*	0.05	-0.01
Asparagine	AA	0.17*	0.09	0.09	0.14	0.07
C2	Acyl-Carn	-0.12	-0.14	-0.18*	0.03	0.01
Methionine sulfoxide	BA	-0.17*	-0.24*	-0.22*	0.05	0.00
Creatinine	BA	0.20*	0.20*	0.19*	0.12	0.04
Acetylornithine	BA	0.08	-0.06	-0.06	0.18*	0.10
PC ae C40:6	GP	-0.04	0.18*	0.11	-0.12	0.13
PC ae C40:2	GP	-0.05	0.19*	0.07	-0.13	0.06
PC ae C40:1	GP	0.08	0.14*	0.14	-0.05	0.07
PC ae C38:6	GP	-0.01	0.11	0.11	-0.04	0.14*
PC ae C38:0	GP	0.03	0.25*	0.18*	-0.14*	0.05
PC ae C36:4	GP	-0.03	-0.15*	-0.07	0.11	0.11
PC ae C36:1	GP	0.02	0.17*	0.07	0.00	0.09
PC ae C34:0	GP	0.02	0.17*	0.06	0.02	0.11
PC aa C42:6	GP	-0.04	0.20*	0.08	-0.17*	0.05
PC aa C40:6	GP	0.02	0.23*	0.18	-0.16*	0.04
PC aa C40:2	GP	-0.04	-0.01	0.03	-0.16*	-0.03
PC aa C40:1	GP	-0.07	0.03	0.04	-0.17*	0.03
PC aa C38:6	GP	0.03	0.22*	0.17	-0.12	0.08
PC aa C38:1	GP	-0.04	0.14*	0.09	-0.11	0.09
PC aa C36:6	GP	0.06	0.27*	0.20	-0.12	0.06
PC aa C36:5	GP	0.01	0.26*	0.16	-0.14	0.02
PC aa C28:1	GP	0.06	0.18*	0.09	0.02	0.08
Lyso-PC a C20:4	GP	0.08	-0.06	0.00	0.14	0.09
Lyso-PC a C20:3	GP	0.14	0.01	0.04	0.16	0.08
Lyso-PC a C170	GP	0.03	0.19*	0.11	0.00	0.09
Lyso-PC a C161	GP	0.06	0.15*	0.09	0.05	0.06
SM (OH) C24:1	SM	-0.05	-0.01	-0.09	0.06	0.14*
SM (OH) C22:1	SM	-0.03	-0.07	-0.10	0.14*	0.12
SM (OH) C16:1	SM	-0.03	0.17*	0.07	0.02	0.15*
SM (OH) C14:1	SM	0.0004	0.15*	0.06	0.07	0.12

Association scores were derived using sparse Partial Least Squares regression. AA, amino acid; Acyl-Carn, acylcarnitine; BA, biogenic amine; GP, glycerophospholipid; PC, phosphatidylcholine; PFHxS, perfluorohexane sulfonate; PFNA, perfluorononanoate; PFOA, perfluorooctanoate; PFOS, perfluorooctane sulfonate; PFUnDA, perfluoroundecanoate; SM, sphingomyelin.

* $P<0.05$

Supporting Table S4. Distribution of metabolites in the clusters of children derived from the integrated latent variables analysis

	Cluster 2	Cluster 1	Absolute difference
Metabolites	**Mean (SD)**	**Mean (SD)**	**in means**
Valine	0.46 (0.29)	-0.19 (0.27)	0.65
Isoleucine	0.48 (0.3)	-0.2 (0.27)	0.68
Leucine	0.45 (0.29)	-0.19 (0.26)	0.64
Tryptophan	0.47 (0.35)	-0.2 (0.34)	0.67
Phenylalanine	0.49 (0.3)	-0.2 (0.25)	0.69
Acetylornithine	0.5 (0.22)	-0.2 (0.2)	0.70
PC aa C36:1	0.46 (0.36)	-0.19 (0.36)	0.65
Lyso-PC a C18:1	0.37 (0.29)	-0.15 (0.3)	0.52
PC ae C36:0	0.36 (0.33)	-0.15 (0.35)	0.51
PC aa C34:1	0.35 (0.34)	-0.14 (0.34)	0.49
Lyso-PC a C20:3	0.33 (0.3)	-0.13 (0.3)	0.46
PC aa C36:3	0.27 (0.37)	-0.11 (0.37)	0.38
H1	0.26 (0.21)	-0.11 (0.21)	0.37
PC aa C36:6	0.22 (0.26)	-0.09 (0.27)	0.31
PC ae C34:1	0.22 (0.33)	-0.09 (0.35)	0.31
PC ae C38:0	0.22 (0.27)	-0.09 (0.28)	0.31
PC aa C32:0	0.21 (0.33)	-0.09 (0.33)	0.30
PC aa C36:5	0.21 (0.23)	-0.08 (0.23)	0.29
Lyso-PC a C20:4	0.2 (0.27)	-0.08 (0.28)	0.28
PC aa C40:6	0.18 (0.23)	-0.07 (0.24)	0.25
PC ae C36:3	0.16 (0.35)	-0.07 (0.38)	0.23
PC ae C36:5	0.15 (0.31)	-0.06 (0.34)	0.21
PC aa C38:6	0.15 (0.25)	-0.06 (0.26)	0.21
SM (OH) C22:1	0.13 (0.22)	-0.06 (0.22)	0.19
PC ae C36:4	0.11 (0.32)	-0.05 (0.35)	0.16
PC ae C38:5	0.11 (0.31)	-0.05 (0.34)	0.16
PC ae C38:4	0.02 (0.33)	-0.01 (0.35)	0.03
SM C18:0	0.02 (0.2)	-0.01 (0.21)	0.03
SM C18:1	0.01 (0.29)	0.00 (0.22)	0.01

***** Mean and SD of metabolites are calculated on $\log_{10}$-transformed and standardized data

Supporting Figure S1. Directed acyclic graph for the association of prenatal PFAS exposure and liver injury risk in childhood

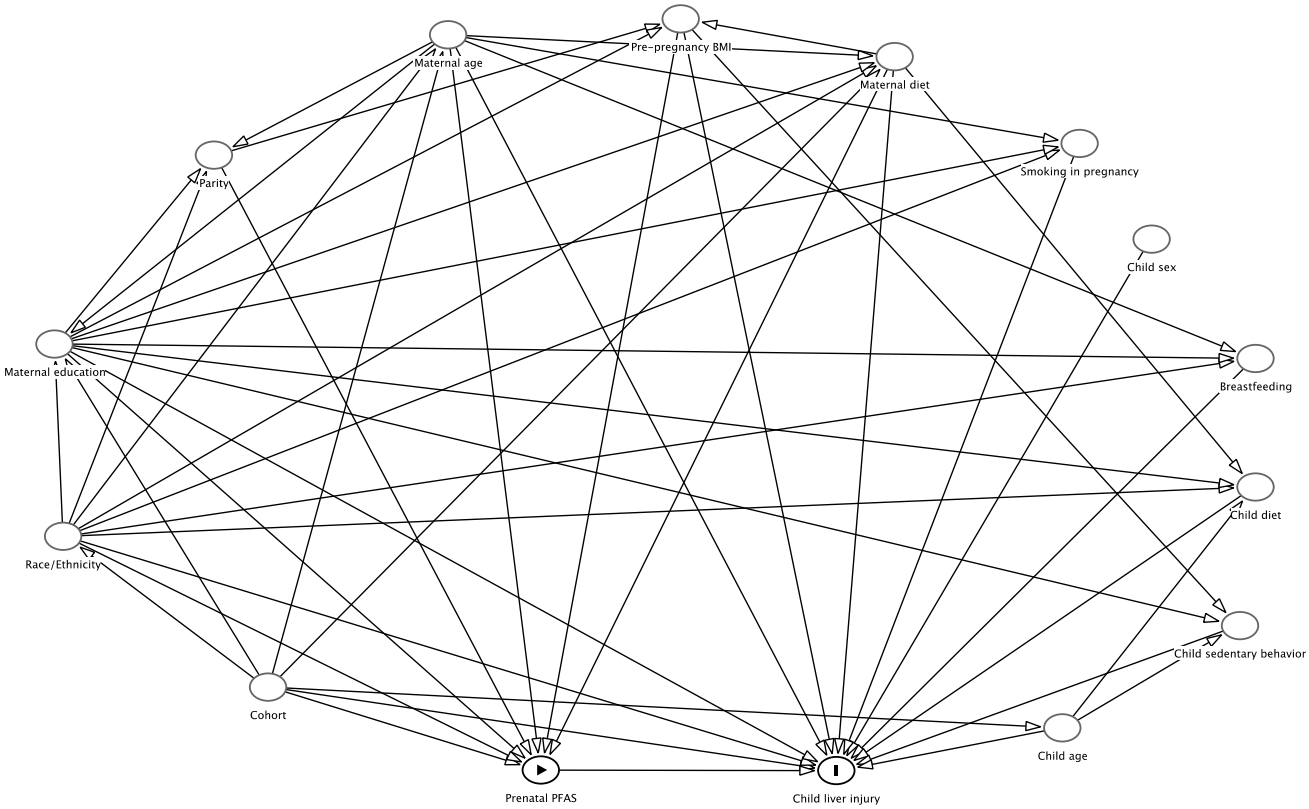

Supporting Figure S2. Associations between single maternal blood PFAS concentrations within the mixture and liver injury risk in children. (a) Exposure–response associations for each PFAS when the other PFAS are fixed at the median. Blue lines represent ORs, gray bands represent 95% confidence bands, and red dotted lines represents the null. **(b)** Exposure–response associations for each PFAS when another PFAS is at either the 25th, 50th, 75th percentile and the remaining PFAS are fixed to their median. Lines represent ORs. Effect estimates were estimated by Bayesian Kernel Machine regression models adjusted for cohort of inclusion, maternal age, maternal education level, maternal pre-pregnancy BMI, child ethnicity, child age, and child sex. PFHxS, perfluorohexane sulfonate; PFNA, perfluorononanoate; PFOA, perfluorooctanoate; PFOS, perfluorooctane sulfonate; PFUnDA, perfluoroundecanoate.

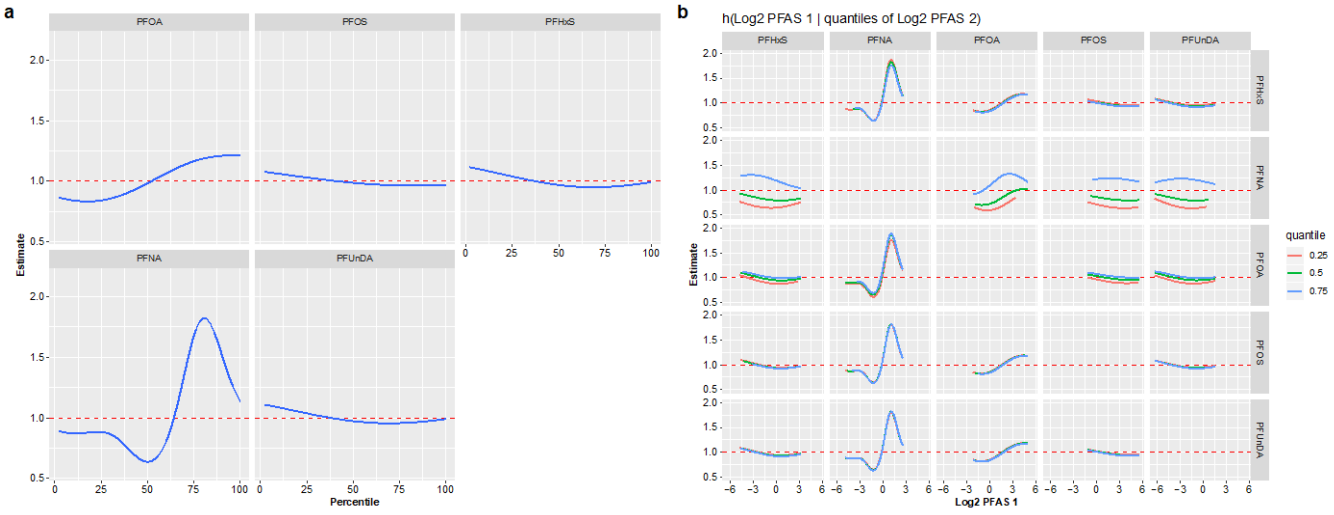

Supporting Figure S3. Joint effect of prenatal PFAS mixture on liver injury risk in sensitivity analyses. (a) Effect estimates after adjusting for child serum PFAS levels. **(b)** Effect estimates after further adjustment for child weight status based on WHO BMI classification. (**c)** Effect estimates after further adjustment for gestational weight gain, food indicators of maternal diet quality, and childhood sedentary behavior and diet quality indicators. (**d)** Effect estimates following exclusion of one cohort at a time and of the two cohorts contributing most to the cases of increased liver enzymes. **(e)** Effect estimates after stratifying for sex. **(f)** Effect estimates after stratifying for gestational period of PFAS assessment. Black circles represent ORs, black vertical lines represent 95% CIs, and red horizontal lines represent the null. Effect estimates were estimated by Bayesian Kernel Machine regression models adjusted for cohort of inclusion, maternal age, maternal education level, maternal pre-pregnancy BMI, child ethnicity, child age, child sex (for a, b and c). For **a**, models were further adjusted for child serum levels of PFOA, PFOS, PFNA, PFHxS and PFUnDA, For **c**, models were further adjusted for gestational weight gain, maternal consumption of fish and fruits and vegetables, child sedentary behavior and child consumption of fish, fruits and vegetables, and sugar-sweetened beverages.